Organo-lined alumina surface from covalent attachment of alkylphosphonate chains in aqueous solution†

Stéphanie Lassiaz,[ab] Anne Galarneau,[a] Philippe Trens,*[a] Dominique Labarre,[c] Hubert Mutin[b] and Daniel Brunel[ad]

Received (in Montpellier, France) 16th December 2009, Accepted 26th January 2010
First published as an Advance Article on the web 18th March 2010
DOI: 10.1039/b9nj00762h

The reaction of octylphosphonic acid with the surface of alumina nanoparticles has been investigated in order to prepare a close packing of grafted-alkyl chains. This goal was attained through a fitting selection of the experimental conditions in terms of pH, reactant amount, reaction time and temperature. DRX, TEM and ^{31}P MAS NMR spectroscopy are all consistent with an efficient covalent anchorage of the alkylphosphonate chains without degradation of the support, demonstrated by the morphology and texture preservation during the modification. In addition to the textural analysis, nitrogen adsorption isotherms provide additional pieces of information on the interaction energy between the nitrogen molecule and the surface. These data, combined with those supplied by the empirical test of floatability of powders (methanol number test), as well as the adsorption properties of the differently functionalized alumina samples using other probes, such as hexane and water, as a function of the chain loading, provided converging information about surface coverage and the hydrophilic/hydrophobic properties of the various materials. Different conformations are proposed to take into account the different results obtained from vapor adsorption measurements.

Introduction

Hybrid organic–inorganic composites have played a prominent role in materials chemistry during the two last decades, even though their design has been sought after for a long time. Actually, the field of hybrid organic–inorganic materials has witnessed tremendous growth due to the potential applications of these tailor-made materials through synthetic sophistication and depth of characterization.[1–3] This is particularly significant in their use as advanced materials for technological applications regarding several fields such as catalysis,[4,5] sorption and separation,[6] optics,[7,8] reinforcement, adhesion and lubrication.[9] They can be also used as sensors,[10] electrodes,[11] or as integrated active nanodevices for clinical testing and model systems for biomembranes.[12]

The different routes to prepare hybrid materials involve the immobilization of organic components into or onto an inorganic support either (i) by trapping in the solid pores, (ii) by tethering to the mineral surface, or (iii) by incorporation in the framework. Among the various designed hybrid organic–inorganic materials,[13] most of them are currently prepared from organosilane and silica precursors.[14] They can be associated by sol–gel processes from organosilane and silica precursors, which allows a high degree of inter-penetration between the two dissimilar phases until intimate mixing at a molecular level.[7,15] Organosilanes as main functionalizing agents for silica have also been used to functionalize other mineral oxide surfaces, such as alumina, on one side,[16] and on the other side, the grafting of silica has been investigated using organophosphonic acid.[17] In the first case, the silane attachment on the AlOH surface has been shown by Pinnavaia and Johnson to be less stable towards hydrolysis than on a SiOH-type surface.[18] That prompted Caro *et al.* to first conceal the alumina surface with a top silica layer, in order to obtain stable hydrophobic ceramic membranes by further silylation treatment with octadecyltrichlorosilane.[19]

Moreover, concerning both cases, the covalent attachment of organic moieties on either alumina or silica using either organosilane or organophosphonate, was firstly achieved by two types of anchorage through Al–O–Si–C or Si–O–P–C bonds, respectively, which require non-hydrolytic conditions because of their instability towards hydrolysis.[20] That explains the absence of Si–O–P bond observation during the treatment of silica with organophosphates.[21] On the contrary, alkylphosphonates formed a permanent hydrophobic layer on titania and zirconia, when these mineral surfaces were treated with an aqueous solution of alkylphosphonic acid,[22] the latter revealing the best ability to produce an ordered monolayer.[23]

[a] *Institut Charles Gerhardt Montpellier-UMR 5253 CNRS/ENSCM/UM2/UM1-Equipe Matériaux Avancés pour la Catalyse et la Santé-Ecole Nationale Supérieure de Chimie de Montpellier, 8 rue de l'Ecole Normale, 34296 Montpellier Cedex 5, France. E-mail: philippe.trens@enscm.fr; Fax: +33 467163470; Tel: +33 467163484*
[b] *Institut Charles Gerhardt Montpellier-UMR 5253 CNRS/ENSCM/UM2/UM1 Equipe Chimie Moléculaire et Organisation du Solide-Université Montpellier 2, Place Eugène Bataillon, 34095 Montpellier Cedex 5, France*
[c] *Rhodia, Centre de Recherches, 52, rue de la Haie le Coq, 93308 Aubervilliers Cedex, France*
[d] *Instituto de Tecnología Química UPV-CSIC, Universidad Politecnica de Valencia, Av. de los Naranjos s/n, 46022 Valencia, Spain*
† Electronic supplementary information (ESI) available: A graph illustrating the evolution of zeta potential as a function of pH. See DOI: 10.1039/b9nj00762h

That prompted many researchers to investigate the surface coverage of both titania and zirconia by alkylphosphonate chains since the last decade, with the aim to study the mechanism of the chain anchorage as a function of the phosphonate precursor and the experimental conditions.[23–25] In this field, Mutin *et al.* have investigated the mechanism of the alkylphosphonate anchorage on titania (anatase) using ^{17}O-enriched organophosphonic acid, demonstrating the bonding mode of the phosphonate anchorage being predominantly tridentate.[26] On the other hand, particular attention was paid to the chain orientation and packing density and to the stability of the Ti–O–P–C or Zr–O–P–C linkage type towards hydrolysis or solvolysis. The most important factor is the formation of different phases coming from dissolution/precipitation processes.[23,25,27–29] In order to overcome this phenomenon, Vioux *et al.* have investigated the alumina functionalization with phenylphosphonate in a two-step process: the first one in an organic medium, using alternative organic-soluble coupling agents such as bis(trimethylsilyl) phosphonate and dialkylphosphonate, and in a second step they add water to increase Al–O–P bond formation.[30] In the case of dialkylphosphonate, this method favored the alumina surface functionalization without the formation of bulk aluminium phosphonate phases. Moreover, the use of dialkylphosphonate in organic media not only excluded the formation of bulk aluminium phosphonate phases, but also allowed control of the surface grafting. In the case of phenylphosphonic acid, they used a mixture of water and methanol at pH 6 to avoid the formation of an aluminium phosphonate phase at room temperature, and reach a density of 4.5 phenylphosphonates per nm^2. At lower pH (pH 4) or higher temperature (reflux), the formation of the aluminium phosphonate phase could not be avoided. No study in pure water has been performed. Although Ramsier *et al.*[31] have shown that methylphosphonic acid in aqueous solution was reacting on an alumina surface, Randon *et al.* have further mentioned that the functionalization of Al_2O_3 membranes with alkylphosphonic acids was unachievable under the conditions used for titanium or zirconium oxide supports, *i.e.*, by using a refluxing aqueous solution of alkylphosphonic acid at 0.1 M for 4 h.[22] Under these conditions, they concluded that the strong reaction of γ-alumina with alkylphosphonic acid probably lead to bulk aluminium phosphonate phase formation instead of simple grafting. However, this behavior is not absolutely clear, as suggested by Öhman *et al.*[32]

The goal of this present work is understand this discrepancy and, therefore, to study in a systematic way the reaction between alkylphosphonic acid and the alumina surface in water at room temperature and to find the best conditions under which the alumina surface can be covered by a self-assembled monolayer of alkylphosphonate without the formation of bulk aluminium phosphonate phases. The alkylphosphonic acid amount, the pH range and the reaction time have been investigated to control the grafting of alkylphosphonic acid on the alumina surface. The resulting materials have been analyzed by various physico-chemical methods to characterize the alumina surface coverage.

Experimental section

Materials

Octylphosphonic acid was obtained as a gift from Rhodia and recrystallized in toluene before use. δ-Alumina—Al_2O_3 C (13 nm particle size; 90 m^2 g^{-1})—was purchased from Degussa and used directly without any treatment. Dichloromethane (Fluka puriss >99.9%) was distilled over calcium hydride. Water was deionised before use.

Grafting of octylphosphonate chains on alumina in aqueous solution

An aqueous solution (70 mL) of octylphosphonic acid was prepared and the pH of the solution was adjusted to pH 6.5 by adding sodium hydroxide 1 M. This solution was then added to a suspension of 2 g of alumina in 80 mL of water in a propylene beaker. The amount of octylphosphonic acid in the first solution corresponded to a defined total loading expressed in density of octylphosphonic molecules per surface unit of alumina (P/nm^2) ranging from 1.1 to 22.9 P/nm^2 (corresponding to 0.06–1.33 g, respectively). The resulting concentration of alumina was adjusted to 50 g L^{-1} by addition of water. The suspension was then stirred at 500 rpm at room temperature for 24 h before centrifugation, except when a specific duration is specified in the kinetic study. The separated solid was washed three times by re-dispersion in 75 mL of deionised water, stirred 20 min each time with centrifugation, then dried under vacuum at 80 °C for 15 h.

Additional grafting was performed without the initial addition of sodium hydroxide to the reaction solution, leading to the natural pH of octylphosphonic acid in water, *i.e.* pH = 2.3, in order to determine the occurrence of any precipitation–dissolution process.

Characterization

Thermogravimetric analyses were performed under dry air from room temperature up to 800 °C at 10 °C min^{-1} on a Netzsch STA 409 PC Luxx thermobalance.

The elemental chemical analyses of the materials were performed by the Service Central d'Analyses CNRS (Vernaison, France). The grafting density of octylphosphonate chains on alumina (P/nm^2) was calculated from the carbon weight content C%, and taking into account the water loss from ATG (xH_2O wt%) by eqn (1):

$$\mathrm{P/nm^2} = \frac{C\% \times L_A}{8 \times 12 \times C\% \times S_{BET} \times 10^{20} \times \left[100 - X\% - \left(\frac{C\% \times M_{C8H17}}{8 \times 12}\right)\right]} \quad (1)$$

where L_A is the Avogadro number, $M_{C_8H_{17}}$ is the molar mass of octyl chains, S_{BET} the surface area (m^2 g^{-1}) of the alumina, with 71 g mol^{-1} being the molar mass of 1/2 P_2O_5.

The uncertainty in the grafting density has been calculated using the uncertainty of elemental analyses and thermogravimetric determination of mass losses.

^{31}P solid-state NMR spectra were obtained with a Bruker Advanced DPX 300 spectrometer, using magic angle spinning

(MAS, spinning rate 10 kHz) and high power proton decoupling; the flip angle was 45° and the recycling delay 10 s. The ^{31}P chemical shifts were referenced to H_3PO_4 (85% in water).

The materials have been labeled according to their content of octylphosphate per nm^2. For instance, P0 stands for the pristine δ-alumina, P47 stands for the δ-alumina grafted with 4.7 octylphosphonate groups per nm^2.

Transmission electron microscopy (TEM) was performed on a Jeol 1200 EX instrument. X-Ray diffraction (XRD) experiments were performed on a Philips X'pert Pro MPD diffractometer used in θ/θ mode with $\lambda(Cu_{K\alpha 1}) = 1.5406$ Å. Zeta potentials were evaluated on a Malvern 3000 Zetasizer (50 mW laser at 644 nm). An aqueous suspension of alumina (1 g L^{-1}) was firstly prepared, and aliquots of 20 mL of this suspension were analyzed after pH adjustment in a pH range $4 < pH < 10$ by adding either HCl or NaOH.

The nitrogen sorption isotherms at 77 K were obtained on a Micromeritics Gemini 2360 apparatus. The solids were dried overnight under vacuum at 120 °C before being analyzed. Surface area and C_{BET} parameter were determined from the BET equation in the range $0.1 < p/p^\circ < 0.3$. The surface coverage of nitrogen molecules was taken as 0.135 nm^2 for a pure alumina surface and as 0.162 nm^2 for organic functionalized alumina, according to Jelinek and Kovátz.[33]

The hexane and water adsorption isotherms at 25 °C were obtained using a home-made apparatus.[34,35] *n*-Hexane, used as sorbate, was provided by Aldrich (purity >99.9%). Water used as sorbate was milliQ water.

The empirical test for the floatability of powders called the "methanol number" (MN) is widely used in the industry.[36,37] MN values can be determined from powder immersion into methanol–water solutions with variable methanol weight percentages from 0 to 70 wt%, after vigorous shaking and examination of the powder floatation after 2 min. MN_{mini} corresponds to the minimum methanol wt% for which some particles start to dive (although most of them are still floating). MN_{max} corresponds to the minimum methanol wt% for which all the particles have drowned. Only MN_{max} will be used in this work.

Results and discussion

Preparation and characterization of the materials

δ-Alumina was chosen in the present work for its physico-chemical characteristics: particle size, particle morphology and surface chemical properties, conferring to it a better chemical stability as compared with other alumina supports. δ-Alumina is one of the most crystalline aluminas, with a relatively high surface area (90 m^2 g^{-1}). Concerning the grafting agent, two advantages of using alkylphosphonic acid instead of silicon derivatives can be detailed. First, the hetero-condensation of alkylphosphonate derivatives with metal oxides is thermodynamically favored, as reflected by the large number of reported crystalline metal (M)-phosphonate phases built from M–O–P bonds. Second, the formation of P–O–Ps bond by homocondensation should not occur in aqueous sol–gel processing through nucleophilic substitution, which arises with silicon derivatives under high temperature dehydrating conditions.[23,29a]

Another advantage of using long chain alkylphosphonic acid, *i.e.* octylphosphonic acid, as coupling molecules instead of alkyl or trimethylsilyl phosphonic ester derivatives is the possibly easier quantitative control of the surface coverage, due to the higher solubility in water of acids compared to esters. Hence, an excess of octylphosphonic acid grafting agent can be used in order to improve the surface coverage of alumina. Furthermore, the advantage of octylphosphonic acid grafting agent compared to other organic functions is the ability of alkyl chains to associate by van der Waals interaction, which generally occurs for alkyl chain lengths greater than eight carbon atoms, and form a self-assembled monolayer (SAM). Octyl chains combine both advantages of high aqueous solubility and lateral chain interaction, which could promote the grafting density. In the case of the surface modification of alumina with alkylphosphonic acids, the literature reports the existence of a balance between the grafting process and the formation of the bulk aluminium phosphonate phases.[19–32] In order to control and to understand the formation of either reaction, we investigated the influence of several parameters such as pH, reaction time and octylphosphonic acid amount.

The XRD of the material shows an intense peak at $\theta = 2.1°$ with two other weaker peaks at $\theta = 4.2°$ and 6.4°, as depicted in Fig. 1. This pattern is characteristic of a lamellar aluminium octylphosphonate structure. Indeed, the interlamellar distance d(100) determined from the peak hkl 100 by means of the formula $d = \lambda/2\sin\theta$ (with $\lambda = 1.5406$) is 21 Å, and the other *d* values d(200) = 10.5 Å and d(300) = 6.9 Å, are characteristic of a lamellar structure with the sequence d(100) = 2 d(200) = 3 d(300). This spacing is consistent with an octylphosphonate bilayer arrangement in the intergallery region of the alumina oxide depicted in Fig. 1.

In a first experiment (sample P62), the alumina particle suspension was simply treated with octylphosphonic acid in aqueous solution for 24 h at room temperature (without pH adjustment). The pH of the solution obtained was pH = 2.1. The solution was containing a large excess of octylphosphonic acid molecules corresponding to 22 molecules per nm^2 of alumina surface. Under these conditions, the resulting material was featuring, after washing and drying, an amount of octyl chains corresponding to 6.2 octylphosphonate molecules per nm^2 (Table 1).

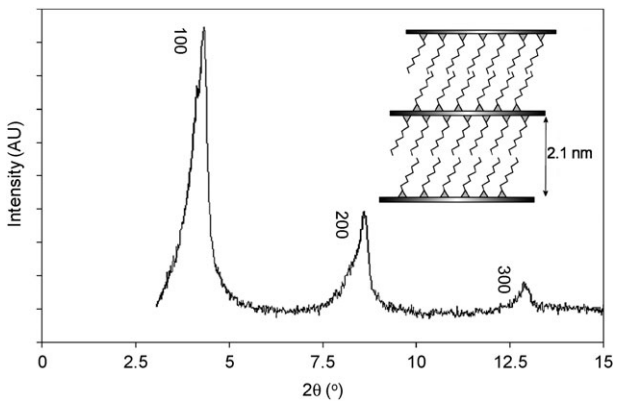

Fig. 1

Table 1 Effect of initial pH on the octylphosphonic loadings. Contacting amounts are related to the amount of octylphosphonic acid grafting agent present in the initial solutions. With the specific surface area of alumina and the mass of sample used, these amounts have been expressed in octylphosphonic acid molecules per nm^2

Sample	Initial pH	Contacting amount P/nm^2	Elemental analysis, %C	H_2O wt loss % (TGA)	Suface loading P/nm^2 (±0.2)
P62	2.3	22.1	7.16	9.0	6.2
P47	6.5	22.9	5.99	3.8	4.7

This spacing is consistent with an octylphosphonate bilayer arrangement in the intergallery region of the alumina oxide (depicted in Fig. 1). The ^{31}P CP-MAS NMR spectrum of the sample P62 is displayed in Fig. 2.

The presence of sharp resonance peaks at 14.5 and 16 ppm exhibited on the spectrum of P62 shown in Fig. 2 is also characteristic of an organized metal–phosphonate phase, in accordance with the lamellar octylphosphonate–aluminium structure previously suggested from XRD analysis (Fig. 1). The TEM pictures of the aluminic phases depicted in Fig. 3 before (nanoparticles of Al_2O_3) and after treatment with octylphosphonic acid (without pH adjustment, sample P62, Fig. 3) reveal a strong solid modification with the appearance of large pellets characteristic of a lamellar phase formation, which confirms the phase transformation. The dissolution/reprecipitation process leading to the formation of the aluminium phosphonate phase with a lamellar structure should very likely be favored by the low pH of the initial octylphosphonic acid solution, which could contribute to alumina dissolution. Hence, we have examined the influence of pH on the reaction.

The solubility of polycrystalline alumina with high structural order, such as cubic close-packed lattice γ- or δ-Al_2O_3, or hexagonal close-packed lattice α-Al_2O_3, determined from the curves of the solubility *versus* pH, has been reported as negligible in the range $4.7 < pH < 8$, except at high ionic strength.[38] However, Carrier *et al.* have shown more recently that γ-Al_2O_3 is thermodynamically unstable in aqueous suspensions, leading to another more stable phase by dissolution/precipitation: gibbsite in acid conditions and/or bayerite in basic conditions.[39] However, this process has been found to proceed at a very slow rate (reaction time greater than 10 h),

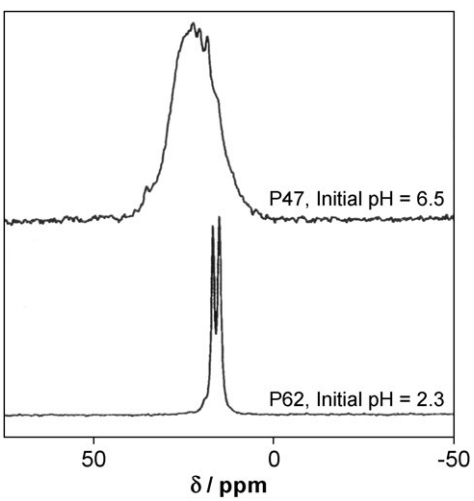

Fig. 2

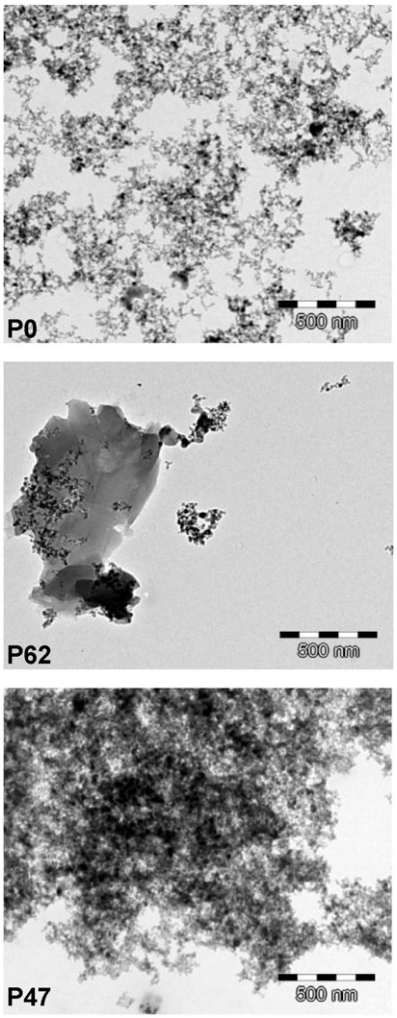

Fig. 3

with a minimum in the solubility profiles at pH = 6.4. Consequently, in this present work, the alumina was further treated with an octylphosphonic acid solution with the same amount of grafting agent for the same reaction time as previously used, but in which the pH had been adjusted to pH = 6.5 by adding sodium hydroxide. The zeta potential curve *versus* pH of the δ-Al_2O_3 used in this work, determined by electrophoresis, features a positive charge of the surface for $4 < pH < 9$, and an inversion of the polarization sign (I.E.P.S.) at pH ~ 9.5 (see ESI Fig. S1†), which is slightly higher than that of different types of alumina, typical of amphoteric solids, which are in the range of $7 < pH < 9$.[40] At pH = 6.5, the alumina surface develops a positive charge and the octylphosphonic species are mostly under an anionic

monocharged form $C_8H_{17}PO_3H^-$; the pK_{a_1} and pK_{a_2} of octylphosphonic acid being 2.1 and 8.1, respectively. Thus, this pH condition should minimize alumina solubilization and favor Coulombic interaction by the opposite charges developed by each component of the couple grafting agent/solid surface.

The resulting material (P47), obtained by pH adjustment to pH = 6.5, exhibits a grafting density of 4.7 P/nm^2 (in accordance with what was found before for phenylphosphonate grafting on alumina in methanol–aqueous media with a density of 4.5 P/nm^2)[30] and did not reveal a noticeable modification of the particle morphology, as shown by the TEM image in Fig. 3.

The XRD pattern of the sample (not shown) did not present any peaks at small diffraction angles, characteristic of a lamellar phase. The ^{31}P CP-MAS NMR spectrum of this sample (Fig. 2) did not exhibit sharp resonance peaks characteristic of an organized aluminium phase, but shows a broad signal with a maximum at 24 ppm. All of these characteristics confirm the grafting reaction of octylphosphonate chains on the alumina surface anchored by different binding modes, and the absence of a bulk alumina phosphonate phase.[30]

Influence of octylphosphonate chain loading on the grafting on alumina

In order to understand the grafting reaction, we have investigated the variation of the surface coverage as a function of the amount of octylphosphonic acid grafting agent present in the initial solution. The surface loadings in octylphosphonate molecules per nm^2 of alumina *versus* octylphosphonic acid amount in the contacting solution (expressed in octylphosphonic acid molecules per nm^2) are reported in Table 2, and the variation of these surface loadings is displayed in Fig. 4. It must be precise that the initial pH of the phosphonic acid solutions was adjusted to pH = 6.5, the final pHs being reported in Table 2. The loading profile shows an increase in the octylphosphonate loading up to a plateau corresponding to ~5 P/nm^2 reached for an amount of octylphosphonic acid in the solution greater than 15 P/nm^2.

This maximum grafted molecule density is in accordance with an alkylphosphonate density found in more drastic conditions (organic solvent, reflux, temperature) for other oxides such as silica, zirconia or titania, and suggests full surface coverage.[41]

For all of the materials, the solid-state characterization confirms the presence of anchored octylphosphonate species on the alumina surface: no XRD peaks have been observed and broad ^{31}P MAS NMR resonance peaks are present. The evolution pattern of the solid-state ^{31}P MAS NMR spectra of materials with different octylphosphonate loadings is shown in Fig. 5. The signal maximum is shifted to lower chemical shift

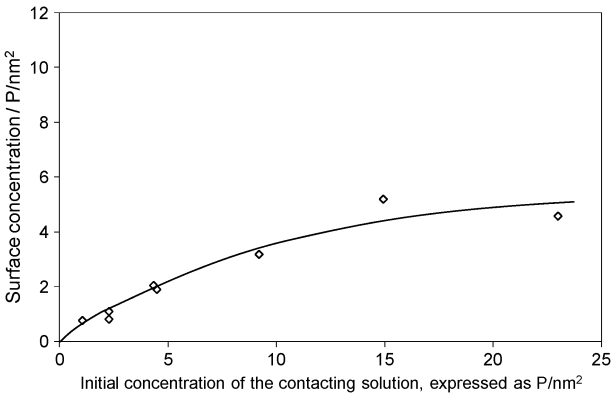

Fig. 4

from 25 to 22 ppm upon increasing loading, and the signal is broadening due to the enhancement of a shoulder at 16 ppm.

This variation suggests a variation in the anchoring mode of the octylphosphonate onto the alumina surface as a function of the loading. In the literature, the ^{31}P MAS NMR signal pattern of interacting phosphonates of SAMs on mineral oxides (ZrO_2, TiO_2, Al_2O_3, Ta_2O_5) has been shown to be the result of a relative proportion of three binding modes: monodentate, bidentate and tridentate.[29a,42,43] For instance, it has been shown that phenylphosphonic acid is bound to the zirconia particles through one, two and three Zr–O–P covalent bonds identified by ^{31}P MAS NMR signals, and are denoted T_1, T_2 and T_3, respectively.[42] The chemical shifts of T_i in Fig. 5 are consistent with those published in many other

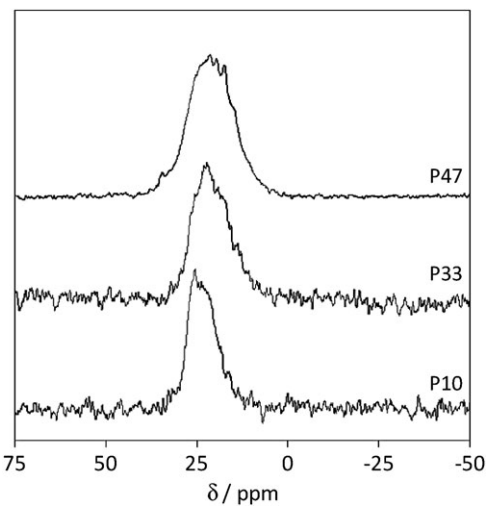

Fig. 5

Table 2 Density of octylphosphonate grafted onto the alumina surface as a function of the initial density of octylphosphonic acid in aqueous solution, obtained by adjusting the initial solution of phosphonic acid to pH = 6.5

Materials	Contacting solution P_{intro}/nm^2	Elemental analysis, %C	wt% H_2O (TGA)	Grafting density P/nm^2 (±0.2)	Final pH
P0	0.0	0.30	2.0	0.0	
P10	1.1	1.59	2.9	1.0	8.5
P22	4.4	3.11	3.1	2.2	8.3
P33	9.2	4.45	2.8	3.3	7.7
P47	22.9	5.99	3.8	4.7	7.4

studies.[26,29a,40,41,45] Likewise, the attachment of self-assembled monolayers of phosphonic acids deposited on titania through several binding modes was argued from the ^{31}P MAS NMR spectrum pattern.[25]

On the other hand, in the case of the anchorage of phosphates onto a titania surface, the monodentate mode has been considered as a likely kinetic intermediate to bi- and tridentate forms and may remain in a certain proportion due to its stabilizing ability *via* hydrogen-bonding with neighbouring bidentate groups.[44–46] However, this assumption, as well as the exact mechanism of binding, is still debated, and likely depends on the nature of the metal oxide.[31,47] Some authors suggest from ^{31}P MAS NMR spectra a preference for a mixed regime of both bi- and tridentate states for alkylphosphonates in SAMs on TiO_2, due to residual detection of P=O and P–OH groups.[20] However, Mutin *et al.* have pointed out the impossible identification of the different phosphorous sites by spectra simulation if only the ^{31}P chemical shifts are considered. The ^{31}P chemical shifts of dodecylphosphonate on a titania surface are at 13 ppm, with shoulders at around 18 and 6 ppm, and would be ascribed to tridentate phosphonate species with different geometries rather than to different modes.[26] In fact, these chemical shifts are sensitive not only to the number of Ti–O–P bonds, each supplementary condensation between P–OH and Ti–OH leading to an upfield shift (displacement towards lower chemical shift), but also to the interaction of the P=O groups with surface Lewis or Brønsted acid sites, which leads to downfield shifts (displacement towards higher chemical shift) and to the variations of the O–P–O bond angles. Nevertheless, by using ^{17}O MAS NMR spectroscopy of enriched ^{17}O phosphonic acid on titania, the authors have demonstrated that the bonding mode, as previously suggested on titania or zirconia,[47] is predominantly tridentate. In our case, from ^{31}P spectra only, we can only suggest that octylphosphonate chains are grafted on alumina, and that the grafting modes of the O–P–O bonds are progressively changing by increasing chain density. The upfield displacement (lower chemical shift) of the signal and the appearance of a shoulder at lower chemical shift could be the result of a higher bonding of octylphosphonate groups on the surface (from mono- to bi- or tridentate), but could also be due inversely to a lower binding from tri- to bidentate due to the removal of the P=O interaction with the surface to give space to the additional molecules approaching the surface.

More recently, a revisited work dealing with high-field ^{17}O MAS NMR spectroscopy associated with simulation enabled the authors to distinguish between Ti–O–P, P=O and P–OH bonds, and to quantify them.[48] They found for dodecylphosphonate chains on titania: 60% Ti–O–P, 20% P=O and 20% P–OH, which would be consistent with a mixture of binding modes of 40% tridentate, 40% bidentate and 20% monodentate species. However, no correlation could be found between the ^{31}P and the ^{17}O MAS NMR spectra. In Table 2, we notice that the pH of the solution increased during grafting from pH 6.5 to 8.5 (for a grafting density on alumina of 2.2 P/nm^2, corresponding to an initial grafting agent amount of 4.4 P/nm^2), as a result of the liberation of OH^- species due to the binding of P–O^- with Al–OH or P–OH with Al–O^-. This grafting density is very close to the maximum found for silica grafted by coating with trimethoxyoctylsilane (2.5 octyl chains/nm^2) leading to a majority of tridentate species.[49] For higher loading (3–5 P/nm^2), the resulting pH after grafting is lower, pH = 7.4, and could be the result of less bindings between P–O^- with Al–OH or P–OH with Al–O^-. This would be in favor of the second hypothesis: with a majority of tridentate species at grafting density up to 2 P/nm^2 and the progressive increase in bidentate species for grafting density greater than 3 P/nm^2. Nevertheless, the lower pH after grafting for higher grafted density could also be the result of the use of a larger amount of octylphosphonic acid, which in this range of pH acts as a buffer solution. In any case, as demonstrated for titania,[48] a mixture of the different kinds of bindings is expected. The study of adsorption of different molecular probes (nitrogen, *n*-hexane and water vapour) on the grafted material's surface might give us an idea of the surface polarity of the materials as a function of the grafting density and, therefore, bring some light about the remaining OH groups on the surface due to residual P–OH of the mono- or bidentate type of grafting.

Kinetic study of octylphosphonate chains grafting on alumina

Before that, to understand the process of grafting, we have examined the evolution of grafting density as a function of reaction time for a starting solution of octylphosphonic acid of 4.6 P/nm^2 (Fig. 6a and b).

Two regimes proceeded during the octylphosphonate loading. The first one was a very fast process, and a plateau corresponding to a number of grafted octylphosphonate molecules of $\sim$1.5 P/nm^2 was reached after a few minutes. Then, the second one was very slow, and an additional grafting corresponding to $\sim$2 P/nm^2 molecules were linearly added over a period of 21 days.

The ^{31}P MAS NMR spectra (Fig. 7) show no sharp resonances at 14.5 and 16 ppm, and XRD reveals no diffraction peaks (not shown), those results demonstrate that in our conditions of grafting (pH = 6.5, room temperature) no dissolution/reprecipitation process occurs even over three weeks of reaction.

The evolution of the ^{31}P NMR spectra as a function of reaction time is very similar to the previous study as a function of the amount of grafting agent, the maximum of the peak ($\sim$25 ppm) is slightly shifted towards lower chemical shift and the peak is broadening by the appearance of a shoulder at lower chemical shift ($\sim$17 ppm). The anchorage modes of O–P–O bonds are changing as a function of reaction time, which is also corresponding to an increase in octylphosphonate chain density, as in the previous study. The existence of the two regimes of grafting process suggests that the higher rate of the first regime would result from a higher local concentration of octylphosphonic acid groups near the alumina surface. An explanation could be, for the first regime, the contact of a micellar organization of the octylphosphonic acids with the surface, leading to the fast grafting of an already interacting molecular assembly. Indeed, the initial concentration of the phosphonic acid is 3.8×10^{-2} mol L^{-1}, which is higher than the critical micellar concentration

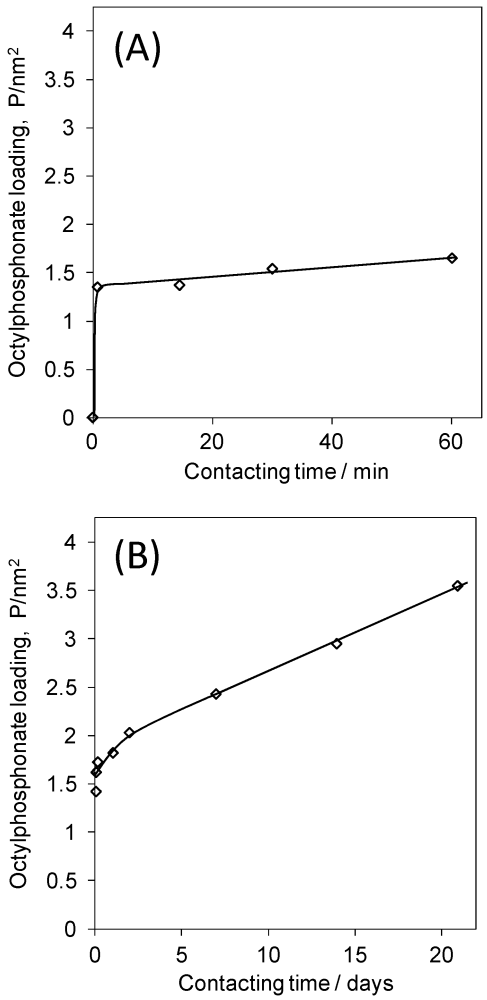

Fig. 6

(cmc $\sim 3.0 \times 10^{-2}$ mol L^{-1} at pH 6.5). When 1.6 P/nm^2 of octylphosphonic acid were anchored after half an hour, the reacting solution concentration decreases to 2.5×10^{-2} mol L^{-1}, which is below the cmc. Hence, the supplementary octylphosphonate chains loading during the second regime would require the addition of single molecules, which is difficult due to both the steric hindrance of the octylphosphonate chains already present on the surface, and the fact that the surface charge becomes less and less positive due to the charge compensation occurring during the grafting process.

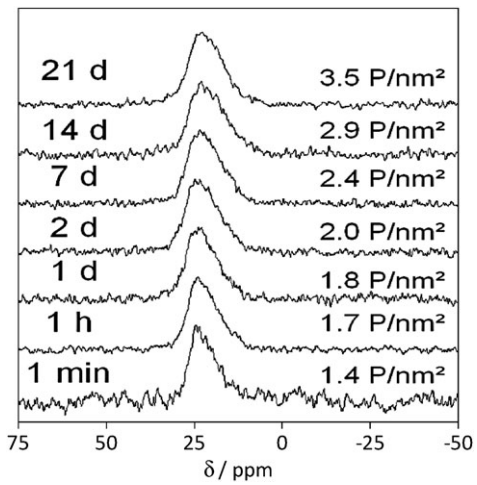

Fig. 7

As revealed by the evolution of the ^{31}P NMR spectra, the addition of molecules in the second process on the alumina surface lead to some restructuring of the binding modes of the already grafted species by shifting the peak maximum to lower chemical shift (Fig. 7). As a hypothesis, we can suggest that tridentate species are first adsorbed and react with the surface and could further break a bond, or displace the interaction of the P═O bond with the surface. This would allow a supplementary octylphosphonic molecule to graft onto the surface, leading to the development of bidentate species. In order to check the remaining polarity of the surface, and therefore, the surface coverage, different probes (nitrogen, hexane and water) have been adsorbed on the different materials (see below). Another way to test the surface coverage by octyl chains is to determine its hydrophobicity. As the materials are constituted of non-porous nanoparticles, a test named the "Methanol Number" has been performed, which quantifies the floatability of powders in aqueous solutions containing different amounts of methanol.

Methanol number test

The contact angle made by a liquid with a solid surface in the presence of a fluid generally characterizes the wetting/non-wetting properties of the system. Thus, the contact angle between a water drop and an ideal flat solid surface is related to its hydrophilicity ($\Theta_Y < \pi/2$) or hydrophobicity ($\Theta_Y > \pi/2$) by the value of its contact angle. Θ_Y is the Young contact angle which is directly given by the equation $\cos \Theta Y = (\sigma_{sf} - \sigma_{sl})/\sigma_{lf}$ where σ_{sf}, σ_{sl} and σ_{lf} are the interfacial tensions of the solid–fluid, solid–liquid and liquid–fluid interfaces, respectively.[50] Unfortunately, this method leads to many misunderstandings, because the exact calculation of the interfacial tensions is questionable in some cases, and because deviation of the apparent contact angle exists from the ideal Young contact angle by the heterogeneous wetting regime.[51] This deviation originates from both the roughness and the chemical heterogeneity of most solid surfaces, as well as the presence of air bubbles trapped in the roughness grooves, under the water drops.[52,53] In order to avoid the pitfalls in the field of measurement and interpretation of contact angles stressed by Marmur,[54] we have chosen to investigate the particle floating on a liquid–air interface consisting of various water–methanol compositions. The variation of the methanol number as a function of octylphosphonate grafted on the alumina surface is reported in Table 3.

The determination of methanol numbers was made on a series of samples prepared from the same pristine alumina without noticeable modification of the texture and morphology of the particle aggregates after surface modification. The variation of their value can be seen as an estimation of the modification of the chemical properties of their surface. Indeed, the variation of the floatability mainly depends on the wettability: the air pockets inside the microcavities of the particles or the microcavities due to particle aggregation

Table 3 Methanol number maximum (MN_{max}), nitrogen C_{BET}, hexane C_{BET}, number of hexane and water molecules adsorbed at monolayer coverage

Materials	Grafting density P/nm^2 (±0.2)	MN_{max}	C_{BET} (nitrogen)	C_{BET} (*n*-hexane)	Adsorbed molecules/nm^2 at V_m[a]	
					n-Hexane	Water
P0	0.0	0	126	18.4	1.8	3.3
P10	1.0	0	39	10.1	1.3	1.6
P22	2.2	40	25	7.9	1.1	1.1
P33	3.3	55	23	6.8	1.2	1.1
P47	4.7	60	23	5.5	1.0	1.1

[a] V_m represents the volume of the physisorbed sorbate monolayer.

mainly depend on the hydrophobicity of the surface.[55] On the other hand, the penetration of liquids inside these cavities also depends on the surface wettabilility.[56] It has been previously shown that contact angle, and thus, hydrophobicity, decreases with the increase of alkyl chains of linear alcohols. Hence, the observed variation in the methanol number as a function of the octyl chain loading can be related by an increase in the hydrophobicity of the surface with the increase of grafted chain density. From Table 3, the hydrophobicity of the material is noticeable for a grafting density of 2.2 P/nm^2, and reaches its maximum for 4.7 P/nm^2.

Nitrogen sorption isotherms at 77 K over octylphosphonate-grafted alumina materials

The variation of the surface polarity of surface-modified mineral oxides as a function of both surface loading and anchorage mode has been particularly analyzed in the case of silane grafted on silica.[47] The C_{BET} parameter, used as a polarity indicator for polarisable adsorbed molecules, such as nitrogen, was calculated from the BET equation, applied in the $0.1 < p/p^\circ < 0.3$ relative pressure range of the nitrogen adsorption isotherm. The C_{BET} parameter is usually expressed as in eqn (3)

$$C_{BET}(N_2) \propto e^{\frac{E_1 - E_L}{RT}} \quad (3)$$

where, E_1 is the adsorption energy (J mol^{-1}) for the first monolayer on the surface and E_L is the adsorption energy of the following layers, which is close to the liquefaction enthalpy of nitrogen (J mol^{-1}). Hence, C_{BET} could quantify the adsorbent–surface interaction, and could be related to surface polarity depending on the surface coverage.[49] This assumption has been further confirmed by the surface contact angle value determined by water intrusion in porous silica, and by comparative adsorption of argon and nitrogen for hydrophobized surface characterization.[57,58] The polar surface of pristine hydroxylated silica usually features a C_{BET} parameter of around 100–110 when adsorbing nitrogen at 77 K. However, onto surfaces totally covered by octyl chains through trichlorooctylsilane or chlorodimethoxyoctylsilane graftings, this C_{BET} value decreases down to 18–20. In the case of mesoporous silica, this corresponds to contact angles of 126 and 128°, respectively, characteristic of hydrophobic materials.[49,57] In the present work, the C_{BET} parameter of the pristine alumina is 126, slightly higher than the value mostly observed for polar surfaces such as hydroxylated silica (Table 3). For a partial surface coverage of alumina corresponding to 1.0 P/nm^2, the C_{BET} value decreases down to 39 and further down to 25 for a higher octylphosphonate surface content of 2.2 P/nm^2, revealing a good coverage of the alumina surface and a relatively high hydrophobicity, although lower than on octylsilane/silica materials for which C_{BET} values of 18–20 are usually found. For higher octylphosphonate chain loadings on alumina (3.3–4.7 P/nm^2), a small decrease of the C_{BET} value can be noticed. This slight difference observed between the C_{BET} parameters of the samples featuring loadings in the range 2.2 and 4.7 P/nm^2 suggests that fewer hydroxyl groups are accessible for nitrogen species for higher loading. This could be interpreted as a higher binding mode of phosphonate at high grafting densities. However, at such high grafting density, and at the very low temperature (77 K) used for nitrogen physisorption, the grafted chains are probably lying on the mineral surface and nitrogen molecules probably cannot access the hydroxyl groups either originating from the phosphonate groups or from the non-modified hydroxyl groups of the surface. At maximum loading, *i.e.* 4.7 P/nm^2 the outermost interface would consist of a dense packing of grafted chains similar to self-assembled systems, such as Langmuir–Blodgett films, even though this interface does not feature a fully ordered system, as it could be expected for octyl chains.

Hence, there is a consistency between the probing of the surface polarity with nitrogen adsorption and with methanol number test, which are sensitive to the same loading ranges: loading between $2.2 < P < 4.7$ P/nm^2 are non-polar and hydrophobic, with a higher (and similar) character of hydrophobicity for materials featuring a grafting density of 3.3 and 4.7 P/nm^2. Larger amounts of octylphosphonate chains on the alumina surface increases the hydrophobicity of the material, but no evidence of the binding type can be deduced from nitrogen adsorption.

Adsorption of *n*-hexane on the phosphonate-modified alumina

The adsorption isotherms for the various phosphonate-loaded aluminas containing phosphonate chains in the range 1–4.7 P/nm^2 are plotted in Fig. 8.

n-Hexane adsorption isotherms at 25 °C over alumina recovered with different densities of octyl chains have quite moderated slopes at the origin, relating to a low heat of adsorption, suggesting a mild *n*-hexane/alumina surface affinity. However, the occurrence of the knees of the sorption isotherms depends on the graft loading. Stronger interaction with *n*-hexane is observed in the case of the pristine alumina surface, while this interaction decreases as the density of octyl chains increases. In the case of the highest grafting studied in

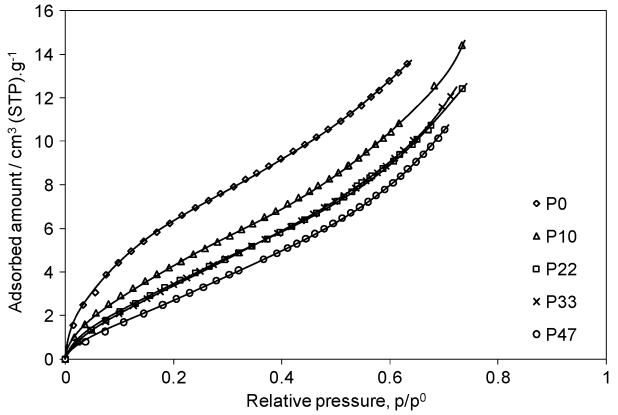

Fig. 8

this work (4.7 P/nm^2), it is almost a linear relationship that can be derived from the sorption isotherm. In other words, the *n*-hexane vapor, used as sorbate, is proportional to the adsorbed amount. This Henry's law type of behavior suggests that the octyl chains act as a solvent for the *n*-hexane species, with the *n*-hexane/octyl chain interaction being very close to the *n*-hexane/*n*-hexane interaction. It is therefore important to distinguish between sorbate/surface interaction and sorbate/surface affinity to understand the results obtained. No saturation plateaus can be obtained, which is not surprising for these absorption processes. In the case of non-grafted alumina, even if no plateau can be observed, a strong inflexion of the sorption isotherm after the knee can be seen. This suggests different sorption processes, the first one being the interaction between *n*-hexane species and the alumina surface with a rather high interaction energy involved, the second one being the sorption of *n*-hexane in a multimolecular fashion.

This difference in terms of sorbate/surface interaction can be ever better seen by plotting the BET transform of the adsorption isotherm in the relative pressure region corresponding to the adsorption through a monolayer/multilayer process (usually $0.15 < p/p^\circ < 0.25$). This may characterize the affinity of a sorbate on a solid surface, as shown using nitrogen. As shown in the past, this determination can prove accurate in the case of *n*-hexane adsorption, even though *n*-hexane is a larger molecule having moreover different possible conformations.[34] Indeed, it was reported that, at low adsorbed amounts, long alkyl chains or polymers first lie down to the surface, and adopt a brush-like structure when reaching the saturation plateau.[59] From these measurements, the mean value of the molecular cross section σ of hexane of 0.514 nm^2 could be derived, allowing the successful determination of textural and surface properties of MCM-41 silica.[60]

As reported in Table 3, the *n*-hexane C_{BET} coefficient of 18.4 for the pristine alumina reveals a higher interaction energy between the hydroxylated alumina surface and *n*-hexane as compared to the *n*-hexane/MCM-41 silica interaction (hexane C_{BET} coefficient of 4–5). With a grafting density of 1 P/nm^2, the C_{BET} coefficient value abruptly falls from 18.4 to 10.1. This suggests that the grafted octyl chains lie on the surface to minimize the surface energy. However, it is not dense enough to cover the whole surface: when the octylphosphonate loading increases, the C_{BET} parameter further decreases (for P22, C_{BET} = 7.9). For higher grafting densities, the C_{BET} parameter does not vary much, which suggests that the hexane molecules mostly interact with the grafted alkyl chains, no longer with the mineral surface. In other words, this suggests the solvation of *n*-hexane species in octyl chains rather than sorption on the alumina surface: when octylphosphonate grafting increases the adsorption process could be replaced by an absorption process.

Scheme 1 illustrates the possible different chain conformations depending on the grafted chain loading. At low loadings (1–2 P/nm^2) the grafted chains/surface interaction could lead to surface coverage by the layered alkyl chain, whereas at high loading (~4 P/nm^2) the potential adsorption sites of the surface could be involved in the phosphonate anchoring bonds.

The number of hexane molecules per nm^2 at the monolayer volume has been determined from the BET theory and eqn (4):

$$n_{hexane} = \frac{V_{ads}^{mono} \times L_a}{S_{BET} \times V_m} \times 10^{-21} \quad (4)$$

n_{hexane} is the number of hexane molecules per nm^2 at the monolayer volume, S_{BET} is the specific surface area determined by nitrogen adsorption (m^2 g^{-1}), V_m is the gas molar volume (L mol^{-1}), V_{ads}^{mono} is the adsorbed hexane volume at the monolayer determined by the BET equation, L_a is the Avogadro number (mol^{-1}). The values of n_{hexane} *versus* graft loading are reported in Table 3.

It is noteworthy that the number of adsorbed hexane molecules per nm^2 at the monolayer volume decreases down to half the value of the pristine alumina from 0 up to 2 P/nm^2. This suggests that the grafted alkyl chains shared in the flat surface-monolayered coverage. From 2 to 4.5 P/nm^2, the number of hexane molecules required for making up the total surface coverage is nearly constant and equal to 1.2 molecules per nm^2, confirming that most of the solid surface is recovered by the alkyl grafted chains. Hence, during *n*-hexane adsorption measurements, the non-grafted alumina surface would be totally hidden by the grafted octyl chains, which themselves are interacting with the original alumina surface with similar sorption energy.

Water adsorption on the phosphonate-modified alumina

Water adsorption isotherms at 25 °C have been analyzed to characterize the hydrophilic properties of the grafted alumina. The adsorption isotherms shown in Fig. 9 present a sharp initial slope indicating a strong interaction of water with the surface, particularly for the pure alumina surface, followed by clearly defined saturation plateaus. At the same relative water pressure $p/p^\circ = 0.2$, the adsorbed volume which corresponds to a monolayer coverage strongly decreases from 10 to 4 mL g^{-1} when the surface loading by the octanephosphonate chain coverage increases from 0 to 2.2 P/nm^2. For higher graftings, there is no noticeable change in the water adsorption.

The adsorption isotherms exhibit the same general shape, indicating similar water adsorption processes regardless of the octylphosphonate surface density. This suggests that water species only interact with the free δ-alumina surface, which decreases in amplitude as grafting increases.

The number of water molecules per nm^2 at the monolayer volume was determined using the same equation as shown previously (eqn (4)) and reported in Table 3. This number falls

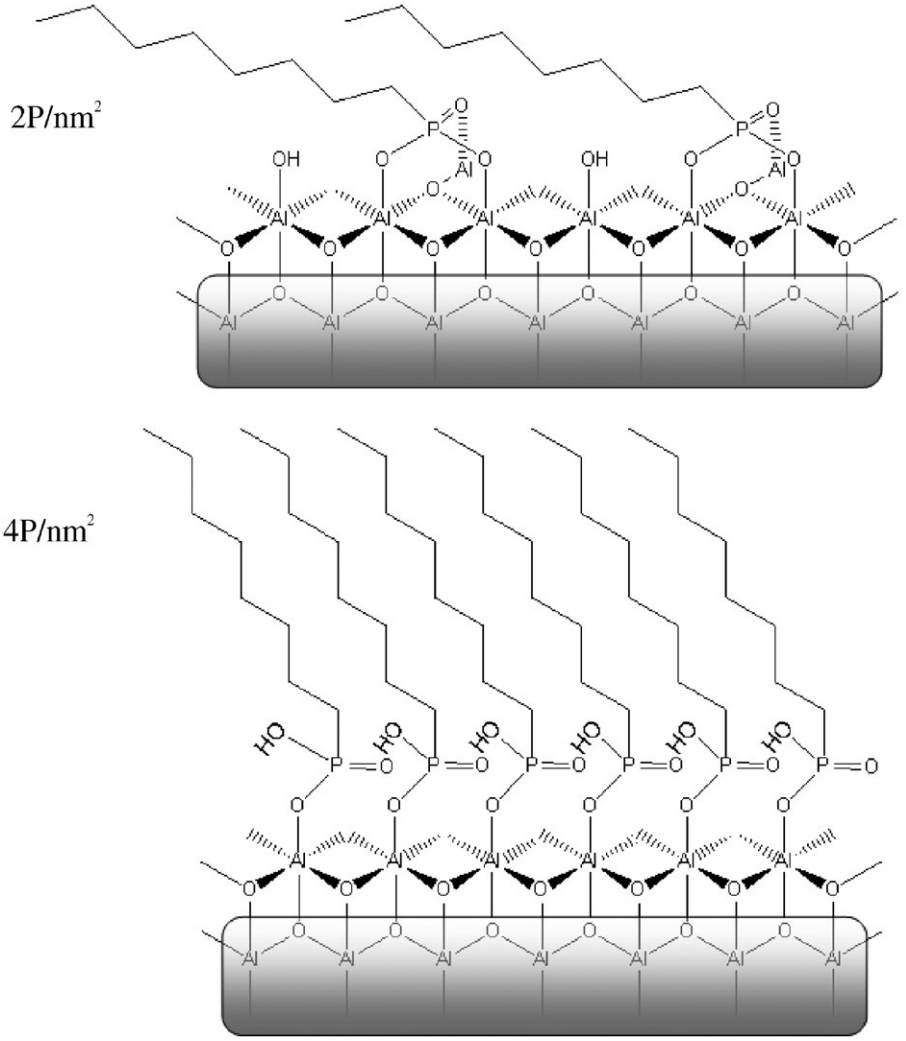

Scheme 1

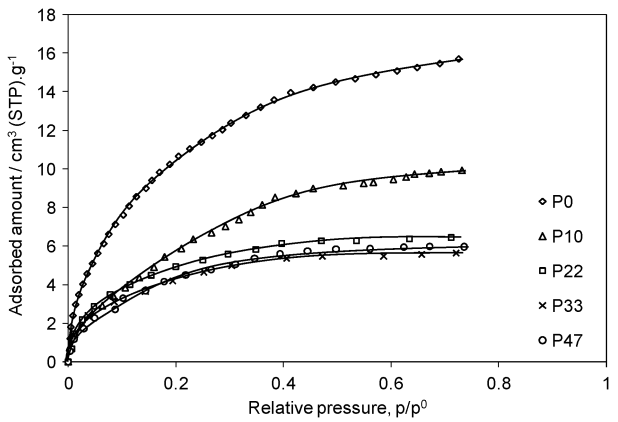

Fig. 9

from 3.3 down to 1.1 H_2O molecules per nm^2 when the grafting of octylphosphonate chains increases from 0 up to 2.2 P/nm^2. This suggests a balance effect between the surface sites for water adsorption and the phosphonate anchoring sites. The water molecules are therefore likely adsorbed on the potential sites for phosphonate grafting. The number of water adsorption sites remains constant at 1.1 per nm^2, even when the grafting density increases from 2.2 to 4.7 P/nm^2. Taking into account this balance effect and the stronger adsorption enthalpy of the water compared to that of *n*-hexane, this suggests that the grafting process at higher loading involves surface Al–OH as well as P–OH or/and P═O non-linked to the surface. This is in line with a modification of the anchoring mode to complete a dense chain loading as suggested previously from the two kinetic regimes of the grafting process.

n-Hexane can interact with the grafted materials in different ways: either with the pristine alumina surface, or with the grafted alumina surface through remaining Al–OH surface sites or even through solvation in the grafted octyl chains. In contrast with *n*-hexane adsorption, the water molecules are able to compete with the alkyl chains flattened on the unmodified surface due their higher interaction energy with the surface adsorption sites.

Conclusion

We have investigated the reaction of octylphosphonic acid with the surface of alumina nanoparticles. The main objective of this study was the hydrophobization of alumina in aqueous

conditions by producing a close packing of grafted-alkyl chains. Although alumina was considered as a not so suitable substrate compared to TiO_2 or ZrO_2, due to the easier formation of bulk alumino-alkylphosphonate phases occurring by dissolution/precipitation processes, this goal was attained through a fitting selection of the experimental conditions in terms of pH, reactant amount, reaction time and temperature. Different methods have been used to characterize the surface modifications of alumina nanoparticles. DRX, TEM and ^{31}P MAS NMR spectroscopy are all consistent with an efficient covalent anchorage of the alkylphosphonate chains with no impairment of the support demonstrated by the morphology and the texture preservation during the modification. In addition with the texture analysis, nitrogen adsorption isotherms provide additional pieces of information on the interaction energy between the nitrogen molecule and the surface. These data, combined with those supplied by the floating test and adsorption properties of the differently functionalized alumina samples using other probes, such as hexane and water, as a function of the chain loading, provided gathering information useful for the surface coverage level and the determination of the hydrophilic/hydrophobic properties of the various materials. In particular, for the highest coverage, the exposed surface is only composed of dense alkyl chains plausibly adopting a brush-like structure. For intermediate coverage, the exposed surface is also hydrocarbonated, which suggests that octyl chains are flattened on the surface due to their interactions with the polar support as driving forces. In contrast to hexane, that cannot compete with the grafted alkyl chains, water molecules are able to substitute the alkyl chain thanks to its stronger adsorption enthalpy. In the case of highest surface coverage of 4.7 P/nm^2, dense monolayered organic chains anchored on alumina provide a chemically stable hydrophobic surface.

Acknowledgements

This work was supported by Rhodia. S. L. also wishes to thank the CNRS and Rhodia for support in the form of a PhD grant.

References

1 B. M. Novak, *Adv. Mater.*, 1993, **5**, 422–433.
2 (*a*) C. Sanchez, B. Julián, P. Belleville and M. Popall, *J. Mater. Chem.*, 2005, **15**, 3559–3592; (*b*) L. Nicole, C. Boissière, D. Grosso, A. Quach and C. Sanchez, *J. Mater. Chem.*, 2005, **15**, 3598–3627.
3 F. Hoffmann, M. Cornelius, J. Morell and M. Fröba, *Angew. Chem., Int. Ed.*, 2006, **45**, 3216–3251.
4 U. Nagel and E. Kinzel, *J. Chem. Soc., Chem. Commun.*, 1986, 1098–1099.
5 (*a*) A. Corma, *Chem. Rev.*, 1997, **97**, 2373–2419; (*b*) D. Brunel, *Microporous Mesoporous Mater.*, 1999, **27**, 329–344; (*c*) A. Stein, B. J. Melde and R. C. Schroden, *Adv. Mater.*, 2000, **12**, 1403–1419; (*d*) D. Trong On, D. Desplantier-Giscard, C. Danumah and S. Kaliaguine, *Appl. Catal., A*, 2001, **222**, 299–357; (*e*) C. E. Song and S. G. Lee, *Chem. Rev.*, 2002, **102**, 3495–3524; (*f*) D. E. De Vos, M. Dams, B. F. Sels and P. A. Jacobs, *Chem. Rev.*, 2002, **102**, 3615–3640; (*g*) Q.-H. Fan, Y.-M. Li and A. S. C. Chan, *Chem. Rev.*, 2002, **102**, 3385–3466; (*h*) Z.-L. Lu, E. Lindner and H. A. Mayer, *Chem. Rev.*, 2002, **102**, 3543–3578; (*i*) A. P. Wight and M. E. Davis, *Chem. Rev.*, 2002, **102**, 3589–3614; (*j*) D. Rechavi and M. Lemaire, *Chem. Rev.*, 2002, **102**, 3467–3494; (*k*) C. Li, *Catal. Rev. Sci. Eng.*, 2004, **46**, 419–492; (*l*) D. J. Macquarrie, in *Nanoporous Materials-Science and Engineering*, ed. G. Q. Lu and X. S. Zhao, Series on Chemical Engineering, Imperial College Press, 2004, vol. 4, ch. 18, pp. 553–595; (*m*) A. Corma and H. Garcia, *Adv. Synth. Catal.*, 2006, **348**, 1391–1412.
6 (*a*) W. A. Aue and C. R. Hasting, *J. Chromatogr., A*, 1969, **42**, 319–335; (*b*) J. N. Kinkel and K. K. Unger, *J. Chromatogr., A*, 1984, **316**, 193–200; (*c*) H. Engelhardt and P. Orth, *J. Liq. Chromatogr. Relat. Technol.*, 1987, **10**, 1999–2022; (*d*) C. P. Tripp and M. L. Hair, *Langmuir*, 1991, **7**, 923–927; (*e*) M. J. Wirth and H. O. Fatunmbi, *Anal. Chem.*, 1993, **65**, 822–826; (*f*) P. van der Voort and E. F. Vansant, *J. Liq. Chromatogr. Relat. Technol.*, 1996, **19**, 2723–2752; (*g*) Y. Bereznitski, M. Jaroniec, M. Kruk and B. Buszewski, *J. Liq. Chromatogr. Relat. Technol.*, 1996, **19**, 2767–2784; (*h*) A. Matsumoto, H. Misran and K. Tsutsumi, *Langmuir*, 2004, **20**, 7139–7145.
7 R. J. P. Corriu, P. Hesemann and G. F. Lanneau, *Chem. Commun.*, 1996, 1845–1846.
8 A. Stein, B. J. Melde and R. C. Schroden, *Adv. Mater.*, 2000, **12**, 1403–1419.
9 (*a*) J. Bjorksten, L. L. Yaege and J. E. Henning, *Ind. Eng. Chem.*, 1954, **46**, 1632; (*b*) J. Soullier, P. Tordjeman and P. H. Mutin, Organic/Inorganic materials, *Mater. Res. Soc. Symp. Proc.*, 2004, **847**, 299–304.
10 (*a*) K. Kimura, T. Sunagawa and M. Yokoyama, *Chem. Commun.*, 1996, 745–46; (*b*) P. Tien and L.-K. Chau, *Chem. Mater.*, 1999, **11**, 2141–47; (*c*) M. Etienne, J. Bessière and A. Walcarius, *Sens. Actuators, B*, 2001, **76**, 531–538.
11 (*a*) G. B. Harper, *Anal. Chem.*, 1975, **47**, 348–351; (*b*) A. Fischer, J. B. Kinney, R. H. Staley and M. S. Wrighton, *J. Am. Chem. Soc.*, 1979, **101**, 6501–6656; (*c*) H. D. Abruna, T. L. Meyer and R. W. Murray, *Inorg. Chem.*, 1979, **18**, 3233–3240.
12 (*a*) J. Livage, T. Coradin and C. Roux, *J. Phys.: Condens. Matter*, 2001, **13**, R673–R691; (*b*) E. Dujardin and S. Mann, *Adv. Mater.*, 2002, **14**, 775–788; (*c*) J. Livage, T. Coradin and C. Roux, in *Functional Hybrid Materials*, ed. P. Gomez and C. Sanchez, Wiley VCH, Weinheim, 2004; (*d*) T. Coradin, J. Allouche, M. Boissiere and J. Livage, *Curr. Nanosci.*, 2006, **2**, 219–230.
13 (*a*) C. Sanchez, G. J. d. A. A. Soler-Illia, F. Ribot and D. Grosso, *C. R. Chim.*, 2003, **6**, 1131–1151; (*b*) M.-A. Neouze and U. Schubert, *Monatsh. Chem.*, 2008, **139**, 183–195.
14 (*a*) E. P. Plueddemann, in *Silane Coupling Agents*, Plenum Press, New York, 1982; E. P. Plueddemann, in *Silane Coupling Agents*, Plenum Press, New York, 2nd edn, 1991; (*b*) G. Arkles, *Chemtech*, 1997, **7**, 766–778.
15 (*a*) K. J. Shea, D. A. Loy and O. W. Webster, *Chem. Mater.*, 1989, **1**, 572–574; (*b*) F. Babonneau, L. Bois, J. Maquet and J. Livage, *Eur. Mater. Res. Soc. Monographs*, 1992, **5**, 319–326; (*c*) K. J. Shea, D. A. Loy and O. W. Webster, *J. Am. Chem. Soc.*, 1992, **114**, 6700–6710; (*d*) R. J. P. Corriu, J. J. E. Moreau, P. Thepot and M. Wong Chi Man, *Chem. Mater.*, 1992, **4**, 1217–1224; (*e*) G. Cerveau, R. J. P. Corriu and N. Costa, *J. Non-Cryst. Solids*, 1993, **163**, 226–235; (*f*) C. Bied, D. Gauthier, J. J. E. Moreau and M. Wong Chi Man, *J. Sol-Gel Sci. Technol.*, 2001, **20**, 313–320.
16 (*a*) S. V. Slavov, A. P. Sanger and K. T. Chuang, *Stud. Surf. Sci. Catal.*, 2000, **130**, 1079–1084; (*b*) A. Sah, H. L. Castricum, A. Bliek, D. H. A. Blank and J. E. ten Elshof, *J. Membr. Sci.*, 2004, **243**, 125–132; (*c*) P. M. Visintin, R. G. Carbonnell, C. K. Schauer and J. M. DeSimone, *Langmuir*, 2005, **21**, 4816–4823; (*d*) V. Szczepanski, I. Valassiouk and S. Smirnov, *J. Membr. Sci.*, 2006, **281**, 587–591; (*e*) M. Kemell, E. Färm, M. Leskelä and M. Ritala, *Phys. Status Solidi A*, 2006, **203**, 1453–1458; (*f*) A. Y. Ku, J. A. Ruud, T. A. Early and R. R. Corderman, *Langmuir*, 2006, **22**, 8277–8280.
17 (*a*) I. Lukeš, M. Borbaruah and L. D. Quin, *J. Am. Chem. Soc.*, 1994, **116**, 1737–1741; (*b*) E. L. Hanson, J. Schwartz, B. Nickel, N. Koch and M. F. Danisman, *J. Am. Chem. Soc.*, 2003, **125**, 16074–16080.
18 L. M. Johnson and T. J. Pinnavaia, *Langmuir*, 1991, **7**, 2636–2641.
19 J. Caro, M. Noack and P. Kölsch, *Microporous Mesoporous Mater.*, 1998, **22**, 321–332.
20 P. H. Mutin, V. Lafond, A. F. Popa, M. Granier, L. Markey and A. Dereux, *Chem. Mater.*, 2004, **16**, 5670–5675.

21 R. Hofer, M. Textor and N. D. Spencer, *Langmuir*, 2001, **17**, 4014–4020.
22 J. Randon, P. Blanc and R. Paterson, *J. Membr. Sci.*, 1995, **98**, 119–129.
23 W. Gao, L. Dickinson, C. Grozinger, F. G. Morin and L. Reven, *Langmuir*, 1996, **12**, 6429–6435.
24 W. Gao, L. Dickinson, C. Grozinger, F. G. Morin and L. Reven, *Langmuir*, 1997, **13**, 115–118.
25 G. Guerrero, P. H. Mutin and A. Vioux, *Chem. Mater.*, 2001, **13**, 4367–4373.
26 V. Lafond, C. Gervais, J. Maquet, D. Prochnow, F. Babonneau and P. H. Mutin, *Chem. Mater.*, 2003, **15**, 4098–4103.
27 G. Guerrero, G. Chaplais, P. H. Mutin, J. Lebideau, D. Leclercq and A. Vioux, *Mater. Res. Soc. Symp. Proc.*, 2001, **628**, CC6.6.1.
28 M. Zwahlen, S. Tosatti, M. Textor and G. Hähner, *Langmuir*, 2002, **18**, 3957–3962.
29 (*a*) P. H. Mutin, G. Guerrerro and A. Vioux, *J. Mater. Chem.*, 2005, **15**, 3761–3768; (*b*) A. Vioux, J. LeBideau, P. H. Mutin and D. Leclercq, *Top. Curr. Chem.*, 2004, **232**, 145–174.
30 G. Guerrero, P. H. Mutin and A. Vioux, *J. Mater. Chem.*, 2001, **11**, 3161–3165.
31 R. D. Ramsier, P. N. Henriksen and A. N. Gent, *Surf. Sci.*, 1988, **203**, 72–88.
32 E. Laiti, P. Person and L. O. Öhman, *Langmuir*, 1998, **14**, 825–831.
33 L. Jelinek and E. sz. Kovátz, *Langmuir*, 1994, **10**, 4225–4231.
34 N. Tanchoux, P. Trens, D. Maldonado, F. Di Renzo and F. Fajula, *Colloids Surf., A*, 2004, **246**, 1–8.
35 P. Trens, N. Tanchoux, A. Galarneau, D. Brunel, B. Fubini, E. Garrone, F. Fajula and F. Di Renzo, *Langmuir*, 2005, **21**, 8560–8564.
36 J. M. Rosen, *Surfactants and Interfacial Phenomena*, Wiley Interscience, New York, 3rd edn, 2004.
37 A. Zdziennicka, *Appl. Surf. Sci.*, 2009, **255**, 7369–7379.
38 (*a*) P. P. Mardilovich, A. N. Govyadinov, N. I. Mazurenko and R. Paterson, *J. Membr. Sci.*, 1995, **98**, 143–155; (*b*) G. Lefèvre, M. Duc and M. Fedoroff, *J. Colloid Interface Sci.*, 2004, **269**, 274–282.
39 X. Carrier, E. Marceau, J.-F. Lambert and M. Che, *J. Colloid Interface Sci.*, 2007, **308**, 429–437.
40 J. P. Brunelle, *Pure Appl. Chem.*, 1978, **50**, 1211–1229.
41 (*a*) H. G. Hong, D. D. Sackett and T. E. Mallouk, *Chem. Mater.*, 1991, **3**, 521–527; (*b*) R. Helmy and A. Y. Fadeev, *Langmuir*, 2002, **18**, 8924–8928.
42 D. Carrière, M. Moreau, P. Barboux and J.-P. Boilot, *Langmuir*, 2004, **20**, 3449–3455.
43 S. Pawsey, K. Yach and L. Reven, *Langmuir*, 2002, **18**, 5205–5312.
44 V. Zoulalian, in *Functionalization of Titanium Oxide Surfaces by Means of Poly(alkyl-phosphonates) Polymers*, dissertation, ETH Zürich, 2008, no. 17618, pp. 19.
45 Y. Chen, W. Liu, C. Ye, L. Yu and S. Qi, *Mater. Res. Bull.*, 2001, **36**, 2605–2612.
46 D. M. Spori, N. V. Venkataraman, S. G. P. Tosatti, F. Durmaz, N. D. Spencer and S. Zürcher, *Langmuir*, 2007, **23**, 8053–8060.
47 C. T. Yim, S. Pawsey, F. G. Morin and L. Reven, *J. Phys. Chem. B*, 2002, **106**, 1728–1733.
48 F. Brodard-Severac, G. Guerrero, J. Maquet, P. Florian, C. Gervais and P. H. Mutin, *Chem. Mater.*, 2008, **20**, 5191–5196.
49 T. Martin, A. Galarneau, D. Brunel, V. Izard, V. Hulea, A. C. Blanc, S. Abramson, F. Di Renzo and F. Fajula, *Stud. Surf. Sci. Catal.*, 2001, **135**, 4849–4856.
50 L. Boruvka and A. W. Neumann, *J. Chem. Phys.*, 1977, **66**, 5464, cited by A. Marmur, *Langmuir*, 2004, **20**, 1317–1320.
51 A. Marmur, *Langmuir*, 2003, **19**, 8343–8348.
52 (*a*) G. Wolansky and A. Marmur, *Colloids Surf., A*, 1999, **156**, 381–388; (*b*) G. E. Yakubov, O. I. Vinogradova and H.-J. Butt, *Colloid J.*, 2001, **63**, 518–525 (*Kolloidnyi Zhurnal*, 2001, **63**, 567–575).
53 (*a*) M. Cournil, F. Gruy, P. Gardin and H. Saint-Raymond, *Chem. Eng. Process.*, 2006, **45**, 586–597; (*b*) M. Nosonovsky and B. Bhushan, *Microsyst. Technol.*, 2006, **12**, 231–237.
54 A. Marmur, *Soft Matter*, 2006, **2**, 12–17.
55 (*a*) O. I. Vinogradova, *J. Colloid Interface Sci.*, 1995, **169**, 306–312; (*b*) O. I. Vinogradova, N. F. Bunkin, N. V. Churaev, O. A. Kiseleva, A. V. Lobeyev and B. W. Ninham, *J. Colloid Interface Sci.*, 1995, **173**, 443–447; (*c*) F. Gruy, M. Cournil and P. Cugniet, *J. Colloid Interface Sci.*, 2005, **284**, 548–559; (*d*) G. E. Yakubov, H.-J. Butt and O. I. Vinogradova, *J. Phys. Chem. B*, 2000, **104**, 3407–3410.
56 G. Kaptay and T. Barczy, *J. Mater. Sci.*, 2005, **40**, 2531–2535.
57 T. Martin, D. Brunel, A. Galarneau, F. Di Renzo, F. Fajula, B. Lefevre, P. F. Gobin, J. F. Quinson and G. Vigier, *Chem. Commun.*, 2002, 24–25.
58 P. Trens, R. Denoyel and J.-C. Glez, *Colloids Surf., A*, 2004, **245**, 93–98.
59 P. Trens and R. Denoyel, *Langmuir*, 1993, **9**, 519–522.
60 D. Maldonado, N. Tanchoux, P. Trens, A. Galarneau, E. Garrone, F. Di Renzo and F. Fajula, *J. Porous Mater.*, 2007, **14**, 279–284.